

RESEARCH ARTICLE | MARCH 11 2024

Simulation and modelling of spray characteristics, spray penetration length and injection pressure of biodiesel

Nur Syuhada Mohd Yaacob; Amir Khalid ✉; Norrizam Jaat; Adiba Rhaodah Andsalier; Muhamad Asri Azizul; Azwan Sapit



AIP Conf. Proc. 2998, 030003 (2024)

<https://doi.org/10.1063/5.0188298>



CrossMark

Boost Your Optics and Photonics Measurements

Lock-in Amplifier

Zurich Instruments

Find out more

Boxcar Averager

Simulation and Modelling of Spray Characteristics, Spray Penetration Length and Injection Pressure of Biodiesel

Nur Syuhada Mohd Yaacob^{1,a)}, Amir Khalid^{1,2,b)}, Norrizam Jaat^{1,c)}, Adiba Rhaodah Andsaler^{1,d)}, Muhamad Asri Azizul^{1,e)}, Azwan Sapit^{2,f)}

¹*Centre of Automotive and Powertrain Technology, Faculty of Engineering Technology, Universiti Tun Hussein Onn Malaysia, Pagoh Education Hub, Johor 84600, MALAYSIA*

²*Centre for Energy and Industrial Environment Studies, Faculty of Mechanical and Manufacturing Engineering, Universiti Tun Hussein Onn Malaysia, Parit Raja, 86400 Batu Pahat, Johor, MALAYSIA*

^{b)} *Corresponding Author: amirk@uthm.edu.my*

^{a)} syuhada_zjanis@yahoo.com.my, ^{c)} norrizam@uthm.edu.my,

^{d)} adiba_rhaodah@yahoo.com, ^{e)} mdasri@uthm.edu.my, ^{f)} azwans@uthm.edu.my

Abstracts. This research compare three different types of Crude Palm Oil (CPO) biodiesel blends, B5, B10, and B15 with different ambient density on nozzle flow and spray characteristics by using CPO and simulated the physics flow pattern of mixture formation with tangential velocity between biodiesel, diesel fuel, and air in the mixing chamber of RCM, to determine the nozzle flow and spray characteristics for different injection pressure of biodiesel spray to ambient variant conditions on mixture formation. In order to mimic the spray processes, an Eulerian-Lagrangian multiphase technique is presented in this study. This work makes use of Computational Fluid Dynamics (CFD) Fluent to examine the spray properties of biodiesel fuels, and the simulation took biodiesel injection into the constant volume chamber of the RCM into account. The boundary condition is set up at a distinct ambient parameter. The presence of in-cylinder flow, the impact of fuel type, injection pressure, and ambient variables on spray behaviour, such as spray penetration, had been examined. Analysis of the spray penetration variation with time for various ambient parameters and different types of biodiesel fuels revealed that the biodiesel fuels were predicted to develop their break-up more quickly due to the fact that all fuels atomize more quickly in the presence of higher injection pressures. The effects of these various parameters were examined in terms of spray characteristics and contrasted with the findings of the experiments.

Keywords: Simulation, Mixture Formation, Spray Characteristics, Biodiesel, Ammonia

INTRODUCTION

The analysis of the experimental findings, simulation and modeling such Computational Fluid Dynamics (CFD) were used to obtain low emission especially Nitrogen Oxides (NOx) complemented with.[1-5] There are three main stages were involved in CFD, which are pre-processing, solver and post processing. Pre-processing involves of geometry and meshing of model in the analysis, where the geometry of drawing of the model can be import from Solid works software. Besides, meshing can identify either the fine or coarse level of mesh [6-9]. CFD software was applied to solve the governing equation and also involving data gathering and visualization of the data and result. The first step in achieving the grid independence test of the spray model is to take into account a constant volume chamber that is focused on the injector and has various grid sizes. Previous experimental findings had shown that the influences of mixture formation on ignition, burning and combustion characteristics[10-13]. After that, the injector and spray chamber geometries mesh, and the flow structure is confirmed. Last but not least, the spray plays an important role in simulating the operation of the engine, with three different injection pressures and a number of ambient conditions [11-16]. Figure 1 and Figure 2 below show the procedure and steps which described in the form

of flowchart regarding the process of CFD. The parameter for this research project is shown in the Table 1. These parameters were considered as the boundary condition in the simulation.

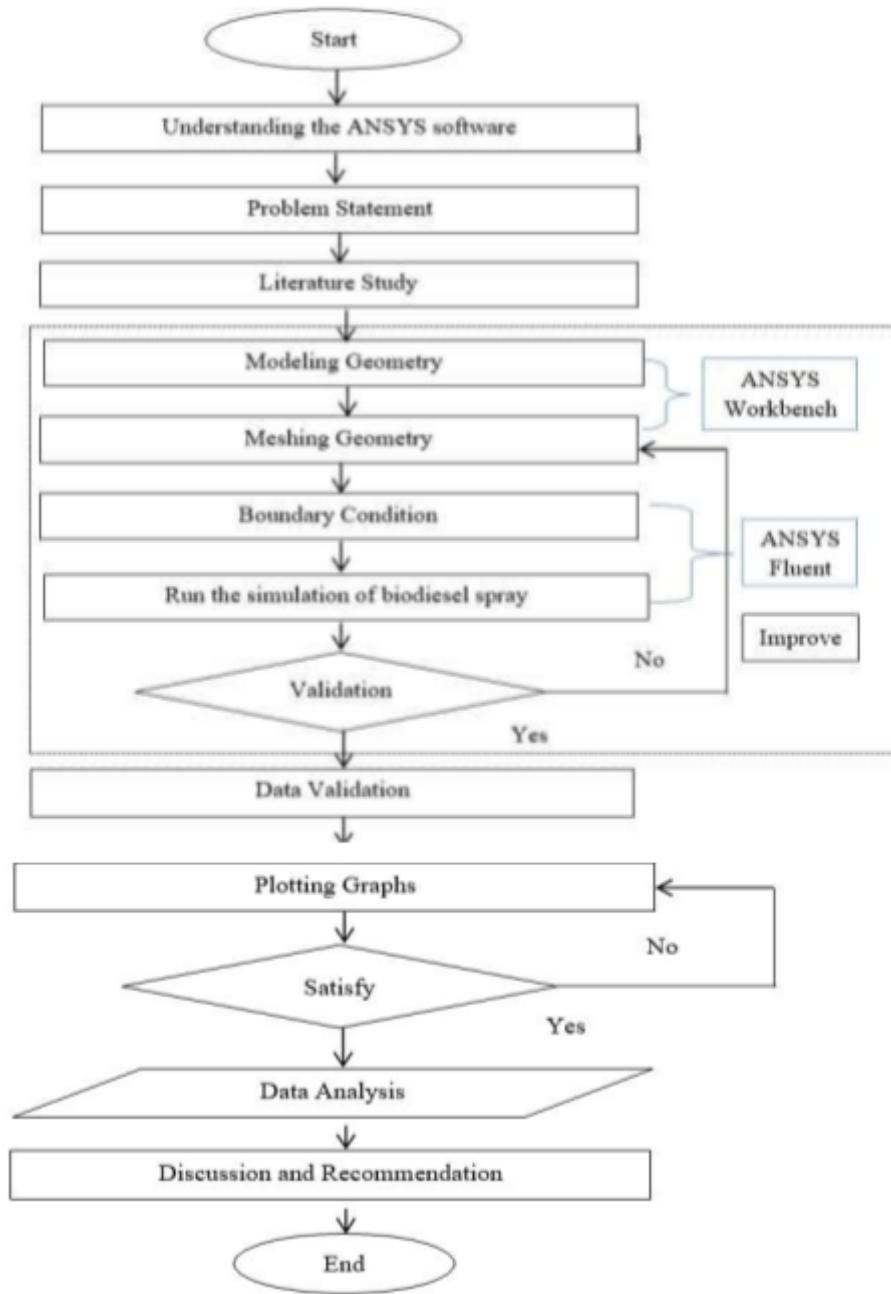


FIGURE 1: Methodology flowchart

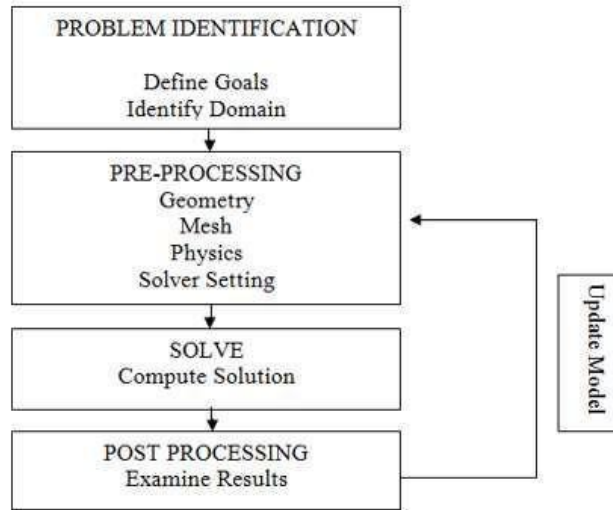


FIGURE 2. Modeling flowchart

TABLE 1. Boundary condition

General	Pressure Based with time velocity formulation	absolution Un-steady
Model	Multiphase volume of fluids (VOF)	Two phases
Turbulence model	K-epsilon model (2 equation)	
Materials	Air	Biodiesel
Boundary Condition	Air-inlet = mass flow rate (kg/s)	Fuel-inlet = mass flow rate (kg/s)
	Atmospheric pressure	Wall = no slip
	Nozzle shape	Cylindrical
	Ambient temperature: T_i Injection 750 K, 850 K, 950 K, 1050 K	
	pressure: P_{in}	100 MPa, 130 MPa, 160 MPa, 190 MPa
Parameters Ambient(Ambient density pressure: ρP)	16.6 kg/m ³ (4MPa)	
	Nozzle injector Hole x diameter: $n_0 \times 25.0 \frac{kg}{m^3}$ (6MPa)	
d_0	33.3 $\frac{kg}{m^3}$ (8MPa)	
Total area, mm	6 × 0.129 (0.0784)	
Fuel properties	CPO biodiesel blends, B5, B10, B15	

BIODIESEL BLENDING

The biodiesel blending machine schematics diagram in figure 3 and figure 4 show the procedure were used to prepare the biodiesel blending process.

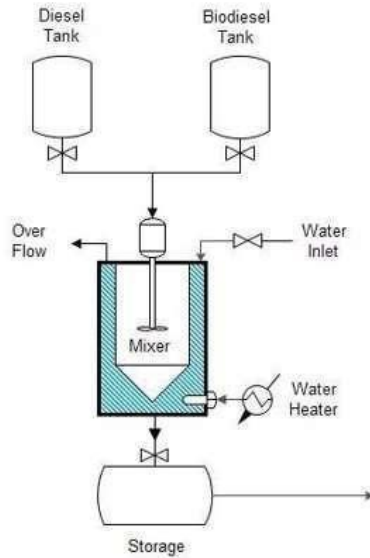


FIGURE 3. Schematics for a biodiesel blending machine

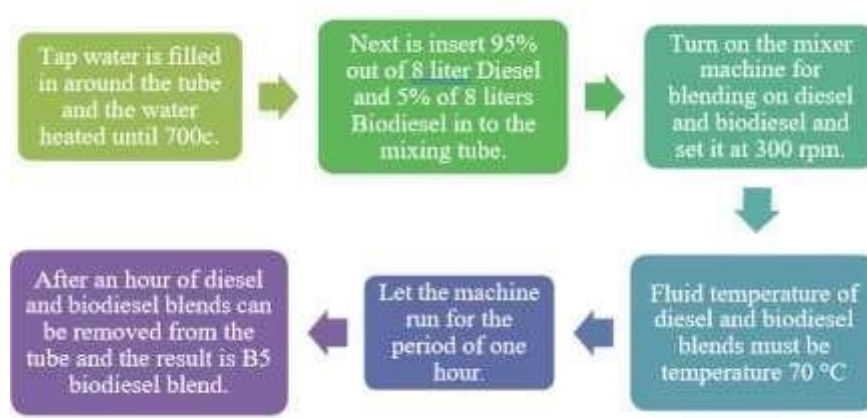


FIGURE 4. Biodiesel blending process

Then, the fuel properties of the fuel were examined based on European Standard for Biodiesel (EN14214) and American Society of Testing Materials (ASTM D6751) as shown in Table 2 to observe properties of density (Mettler Toledo Diamond Scale modelled JB703-C/AF, kinematic viscosity (time taken by a volume of sample (liquid form) to flow under gravity through a calibrated glass capillary viscometer), water content, acid value and flash point test. Volumetric KF titrator model v20 PenskyMartens PMA 4. Based on the properties, the diesel fuel at the first rows shown that density was the lowest but good in kinematic viscosity and low flashpoint observed and make the water content also the lowest value. Second rows from the table is increasing density up to 0.837048g/cm³, promoted flashpoint also high at 91.5C and the water content level up to 120.1 ppm. Comparing between B10 fuel and B15, it seems that the density of B15 was the highest at value 0.840428g/cm³ while the density value of B10

0.837664g/cm³. B15 is observed through density, kinematic viscosity, flashpoint and water content. It is assumed that high density effects the value of kinematic viscosity, flashpoint and water content.

TABLE 2. Physical properties of blended biodiesel fuel

Fuel Properties				
Fuel	Density (g/cm ³)	Kinematic Viscosity (cP)	Water Content (ppm)	Flashpoint (°C)
DIESEL	0.8337	3.0	79.9	80.0
B5	0.8370	3.0	120.1	91.5
B10	0.8376	2.9	158.6	92.0
B15	0.8404	3.0	219.0	93.5

RAPID COMPRESSION MACHINE

The standard diesel combustion was produced using a rapid compression machine (RCM) over a wide range of temperature, pressure, and swirl velocities. A schematic diagram of the RCM and a diagram of the fuel injection system are shown in Figure 5. The RCM has a disc type combustion chamber with a diameter of 60 mm and width of 20 mm. The injector nozzle and spray chamber were applied in these experiments. For the fuel injector design with six orifice holes, it is necessary to save in IGES file and import as geometry modelling in ANSYS Fluent 16.1.

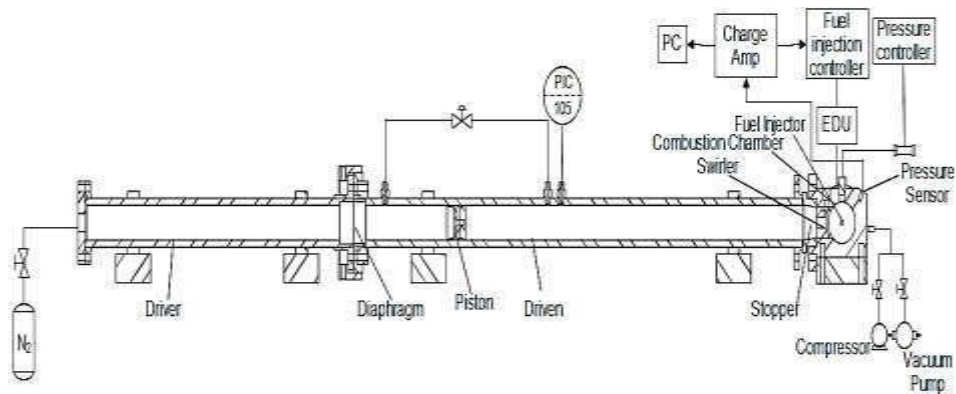


FIGURE 5. Experimental setup of RCM

GEOMETRY OF INJECTOR AND SPRAY CHAMBER

Model for nozzle spray is designed in Solid works software before run the simulation. The spray on nozzle holder is designed in tandem with a constant volume chamber for an easier installation. It observed that Figure 6 full installer and cross-sectional model for the nozzle injector in the constant volume chamber. Arrows may apply to indicate the areas to be analyzed using the Computational Fluid Dynamics (CFD). It is observed that all dimensions are in millimeters and the design of injector shown that is only focus on the injector head and spray chamber. A complete injector has six nozzle was performed with angle of 15 degree between each hole. In order to minimize the error during the simulation, the injector and spray chamber were cut into one per six pieces which only one nozzle hole was left.

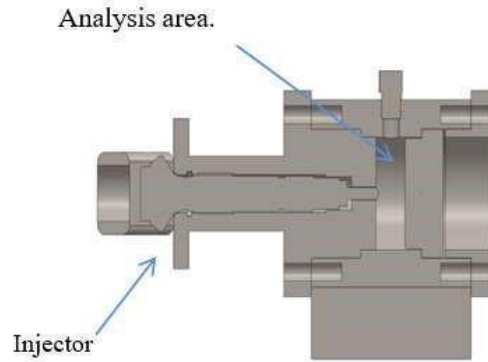



FIGURE 6. Nozzle injector in constant volume chamber: entire and cross-sectional models.

INJECTOR

Table 3 displays the specifications for the injection spray employed, which is from the Bosch design. Figure 7 depicts the design of the injector spray nozzle and the specifications are given in table 3 are diameter nozzle 7mm, diameter hole 0.10mm, number of holes are 6, angle spray is 158, pressure 100Mpa and Toyota Hilux 2.5TD was used.

TALE 3. The specifications for nozzle injection spray

Part manufacturer	Denso
Image	
Diameter nozzle (mm)	7
Diameter hole (mm)	0.10
Number of holes	6
Angle Spray (°)	158
Pressure (MPa)	100
Uses	Toyota Hilux 2.5TD

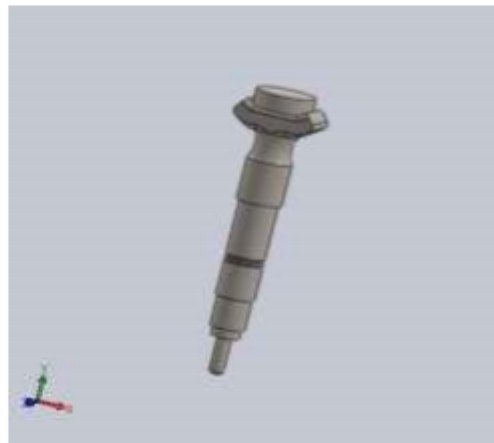


FIGURE 7. The design of the injector spray nozzle PRE-PROCESSING

IN THE INJECTOR OF SPRAY CHAMBER GEOMETRY

Figure 8 depicts the geometry of a mesh part in FLUENT. The geometry acquired for one-sixth of a nozzle injector in the constant volume chamber is adequately meshed using a hybrid mesh and sized using the optimum grid size determined in the previous section. The injector of spray chamber geometry has a maximum cell count of 836547 cells.

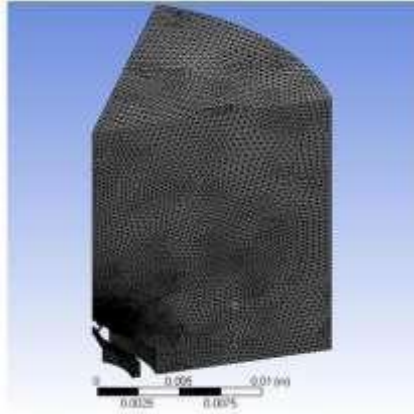


FIGURE 8. 1/6 nozzle injector mesh geometry in constant volume chamber

BOUNDARY CONDITIONS

Boundary is known as the condition where the fluid and air enter or leaves the injector. The application of these conditions must be set as the pressure at inlet, velocity of fluid flow, and the temperature, heat transfer may occur on the wall of injector. 3D model is required for the boundary condition of inlet and outlet channels for ANSYS FLUENT software. Mass flow rate of the inlet was performed to determine the scalar properties and velocity and mass flow of that inlet wall boundaries. Furthermore, the pressure outlet was applied to determine the scalar properties and velocity and mass flow of the flow at inlet wall boundaries. Moreover, pressure outlet was used to determine the static pressure at the outer flow. Besides, the wall boundary conditions are used to determine the characteristic of the wall in geometry during the simulations. Lastly, it is observed that the temperature must be kept at 27°C which is the room temperature. The boundary conditions required in three boundary conditions which are inlet (mass flow rate inlet), outlet (pressure outlet) and solid wall (wall). Comparison between inlet (mass flow rate inlet) and outlet (pressure outlet) as shown in Figure 9 and Figure 10. It can be seen that inlet selection for this case is mass flow rate enters the domain, the mass flow rate can be identified. Different mass flow rates in one inlet noticed that alternative fuel and the air flow in with swirling motion. While the pressure outlet will be set at the surface of triangular prism in which is parallel to the surface of nozzle, outlet pressure is significant to the ambient pressure. It indicates that the flow will come out when going through the nozzle hole of the injector that had been created in the domain. Figure 10 shows the pressure outlet which is located at the opposite site of inlet flow and the bottom of chamber.

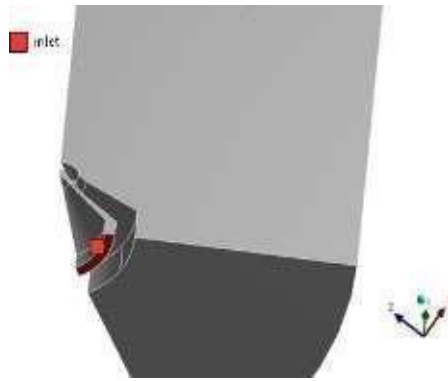


FIGURE 9. Inlet boundary for injection pressure



FIGURE 10. Pressure outlet of the injector

Figure 11 shown that solid wall as part of boundary. Solid wall is the basic boundary conditions that exist in the domain of fluid flow. It noticed that there is no motion in this case because of the shear condition of wall is non-slip for the fluid flow, therefore the wall of injector, nozzle and spray chamber are at stationary wall.

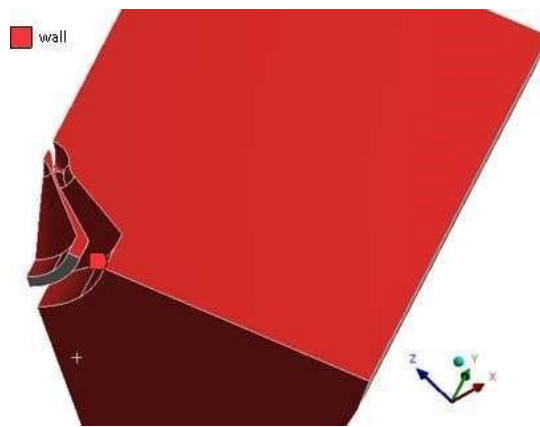


FIGURE 11. Wall of injector being set

SIMULATIONS

Software of ANSYS FLUENT version 16.1. was applied in simulation. In order to evaluate simulation process, three different cases with different nozzle but boundary condition for three nozzle geometries are same throughout the whole simulation process. It is important to import cylindrical orifice diameters into ANSYS software for analysis. It indicates that multiphase volume of fluid (VOF) uses as multiphase liquid where a mixture of a fluid considered as a fluid which has various viscosity and density. Researcher studied two- phase fluid mixing known as biodiesel mixed with air. Simulations use implicit scheme for volume fraction parameter, using a constant mass flow rate on biodiesel phase and air. The calculations for mass flow rate of biodiesel and air in attached in the appendix A. It notices that nozzle design geometries applied referring to the experimental design, nozzle length with 2mm and 0.129mm of nozzle's diameter. Amir Khalid et al. investigated the effects of preheated fuel on the mixture formation of biodiesel spray by using CPO biodiesel by transesterification from the Universiti Tun Hussien Onn Malaysia biodiesel pilot plant. The result as shown in Table 4. The properties of STD and blending ratio biodiesel at ambient temperature. This study conducted using various pressure and temperature constant volume chamber and the properties consist of oxygen content in the biodiesel has a strong effect to the ignition delay. Table 4 presents B40 fuel has the highest value of flashpoint as 100C and also highest value water content as 558ppm. Comparison between B15 fuel and B25 fuel were studied as density value of B25 0.841172 higher than B15 0.840428. It can be seen that both fuels have same kinematic viscosity value 3cP. B25 shows higher at value of flashpoint and water content. It is assumed that high value of density accelerates the value of flashpoint and also water content.

TABLE 4. Standard Diesel Properties and blending ratio biodiesel at ambient temperature [1]

Type	Biodiesel Fuel Properties			
	Density (g/cm ³)	Kinematic viscosity (cP)	Water content (ppm)	Flash-point (°C)
Standard	0.8337	3.0	79.6	80.0
B5	0.8370	3.0	120.1	91.5
B10	0.8376	2.9	158.6	92.0
B15	0.8404	3.0	219.0	93.5
B20	0.8411	3.1	294.7	94.5
B25	0.8417	3.0	363.3	97.0
B30	0.8458	3.2	397.1	97.5
B35	0.8448	3.4	426.9	99.5
B40	0.8482	3.2	558.0	100.0

PROCEDURE FOR A COMPLETE SIMULATION BY USING ANSYS FLUENT

A researcher studied basic procedural steps by using ANSYS Fluent to conduct a simulation as shown below:

- (a) Define the wanted computational domain geometries which used in the simulation.
- (b) Created or imported the model geometry into the Workbench and grid generation
- (c) Suitable solver is defined and set up with appropriate physical models are selected.
- (d) The solution is computed and monitored.
- (e) Results are examined and saved.

GRID INDEPENDENCE TEST

Formerly, grid independency tests in simulation in order to ensure that the discretization errors are relatively small and also to optimize the grid size in the engine simulation. Furthermore, the influence of geometry has to be considered in the accurate and correct geometry. A significant effect on the convergence and predicted results [2, 3,

4] sensitivity was tested on the model with different grid sizes. It has been reported that grid size has a significant effect on the convergence and predicted results [4, 5]. The grid size divided into three levels which are coarse, medium and fine grids with different level smoothing set such as low, medium and high. The simulations were performed on a 6 (holes) x 0.129mm (hole-diameter) x 0.0784 mm of injector in the constant volume chamber with similar condition as the experiments [6]. Table 5 shows three different sets of grids, each with a different number of elements and nodes. It shows the amount of elements and nodes for each group of grid sizes. Furthermore, the number of elements ranges from 836547 to 2550607 elements. By climbing the level of grid sizes from coarse to fine and also the level of smoothing from low to high, the number of elements presents the results is evidently directly related to the number of nodes.

TABLE 5. Different grid sizes with its number of elements and nodes

Grid Sizes	Number of Elements	Number of Nodes
Coarse	836547	154734
Medium	1693577	311968
Fine	2550607	469202

Figure 12 depicts the findings for a spray injection pressure of 100 MPa with three different meshes. It can be shown that 0.8 million cells considerably overestimate the velocity. Furthermore, the domain with more than 1.0 million cells slightly overpredicts velocity when compared to the other grids. The velocity of nozzle obtained is measured by applying a line from the nozzle inlet to outlet which can be seen in the figure below. The data shows that the flow of velocities based on their grid size are corresponding to each other and these grids is in an independence state which means the mesh density can be used for the other grid size. The sudden increase velocity from the fuel inlet as shown in the Figure 12 is believed that the rapid fuel- air mixing occurs at this area. The velocity is decreased as shown in the Figure 10 is due to the loose of energy caused by the rapid mixture formation of biodiesel fuel and air. We found from this data that, in the case of a high injection spray model, the domain should be meshed with 836547 elements or finer to avoid any grid size effects on velocity. The best grid size for the remaining computations is 836547, with the largest grid size set to 'coarse' in the engine model's chamber.

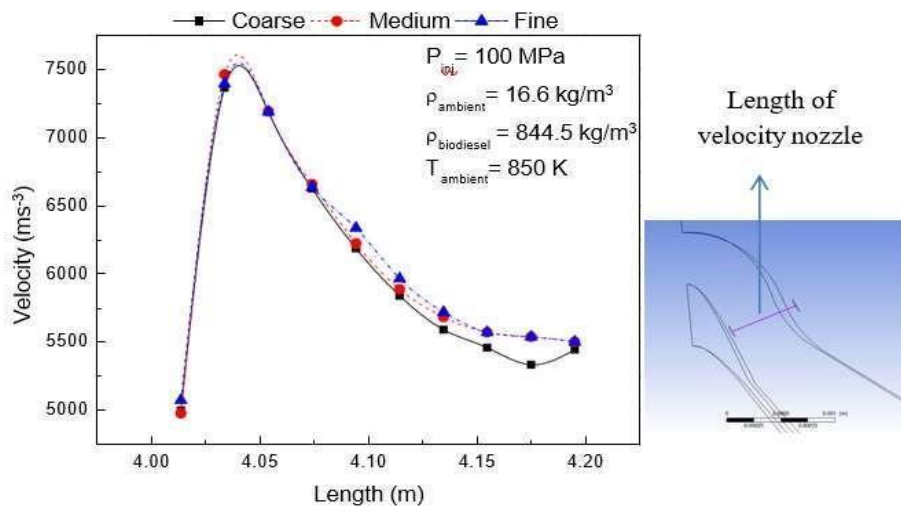


FIGURE 12. Graph of mesh velocity of nozzle over length from inlet to outlet of nozzle.

VALIDATION

It can be seen that Computational fluid dynamics (CFD) was also broadly applied in the prediction of spray penetrations. In order to validate the CFD analysis result with the experimental result, comparison between the experimental and CFD simulation are performed via image processing method using RCM. Meanwhile, a CFD analysis between the simulation and experimental results was conducted to fulfill the purpose of validation. The validation is predictable to ensure that the techniques applying in the simulation is highly accurate. The experiment has been carried out with standard biodiesel fuel, density 844.5 kg/m^3 at equivalent ratio equal to 0.03. The simulation results of spray penetration length are being considered to compare with the experimental data for validation. There are two graphs of results as to predict the validation is valid with error below 3%. Figure 13 shows the graph of 3000 iterations in injection pressure 130 MPa, ambient pressure of 4 MPa and ambient temperature of 850 K. In a few circumstances the simulation may end at 1002 iterations before it could finish all the 3000 iterations, which also meant the solution had converged at 1002 iterations. The normal and expected behavior is seen in the graph as the residuals will repeat the saw tooth pattern until the iterations are complete.

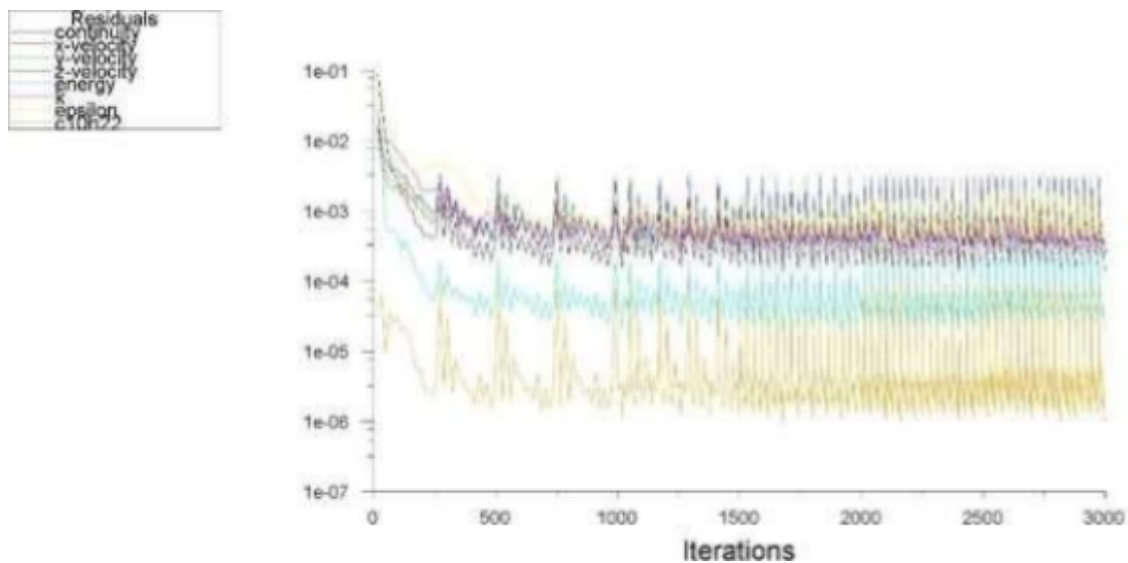


FIGURE 13. Graph of 3000 iterations.

Figure 14 shows the comparison of spray penetration length as the injection pressure is varied. The figure shows the difference between simulation and experimental data is in almost similar pattern in which the average difference for the spray penetration is around 2.89%. Meanwhile graph comparison of ignition delay as ambient temperature is varied is shown in Figure 15. The average difference for the spray penetration is around 2.78%. Thus, the simulation validation can be accepted.

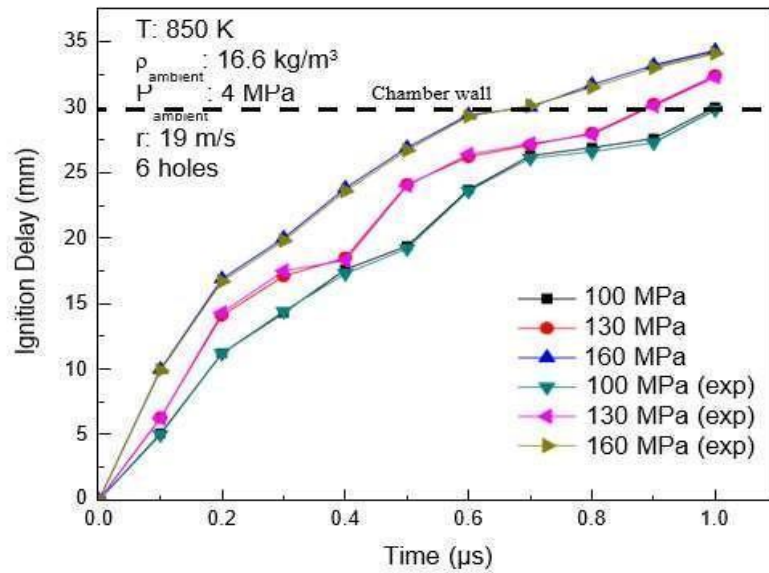


FIGURE 14. Comparison of spray penetration length as the injection pressure is varied

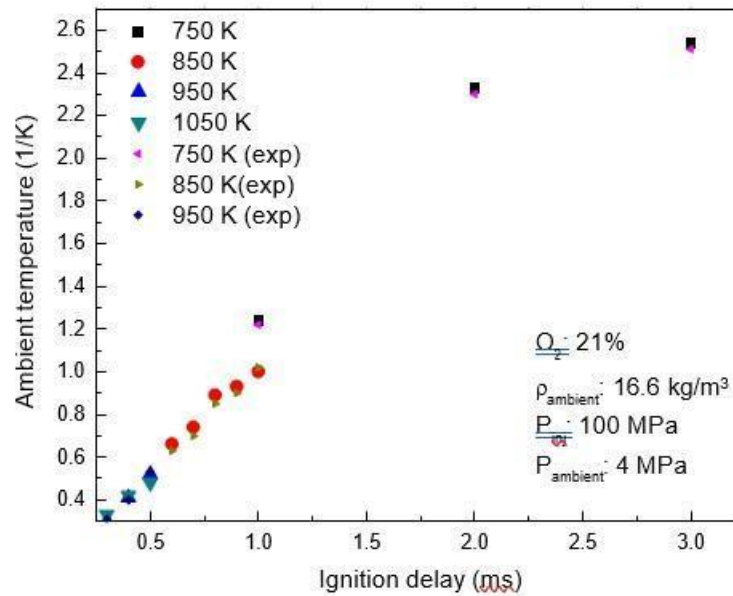


FIGURE 15. Comparison of ignition delay as ambient temperature is varied

CONCLUSIONS

The effect of mixture formation in variant ambient condition and injection pressure of biodiesel spray will be predicted such as the angle of spray cone, the characteristics of area of injection and the spray tip penetration by using difference number of pressures will be retrieved.

The analysis of nozzle flow and droplet size shows that the characteristics of biodiesel spray can be determined during the ignition delay period in which focus on the biodiesel spray during ignition delay. The ignition delay is

expected to be longer as the compressed air temperature and pressure with the temperature being considered are in higher ambient condition.

ACKNOWLEDGEMENT

The authors would like to thank the Ministry of Higher Education (MOHE) for supporting this research under the Fundamental Research Grant Scheme No. FRGS/1/2020/TK0/UTHM/02/21 Vot K307 and also Research Fund Universiti Tun Hussein Onn Malaysia (H802).

REFERENCES

1. Khalid A., Yohan C., Jaat M., Zaman I., Ali M. F. M., and Manshoor B. (2013). Effect of Preheated Fuel on Mixture Formation of Biodiesel Spray. *Applied Mechanics and Materials*, Vol. 393, p. 493498.
2. Andsaler, A.R., Khalid, A., Adila Abdullah, N.S., Sapit, A., Jaat, N., "The effect of nozzle diameter, injection pressure and ambient temperature on spray characteristics in diesel engine", (2017) Journal of Physics: Conference Series, 822 (1), art. no. 012039.
3. Khalid, A., Azman, N., Zakaria, H., Manshoor, B., Zaman, I., Sapit, A., Leman, A.M., "Effects of storage duration on biodiesel properties derived from waste cooking oil", (2014) *Applied Mechanics and Materials*, 554, pp. 494-499.
4. Jaat, N., Khalid, A., Mustaffa, N., Zulkifli, F.H., Sunar, N.M., Nursal, R.S., Mohamad, M.A.H., Didane, D., "Analysis of injection pressure and high ambient density of biodiesel spray using computational fluid dynamics", (2019) CFD Letters, 11 (1), pp. 28-39.
5. Khalid, A., Mudin, A., Jaat, M., Mustaffa, N., Manshoor, B., Fawzi, M., Razali, M.A., Ngali, Z., "Effects of biodiesel derived by waste cooking oil on fuel consumption and performance of diesel engine", (2014) *Applied Mechanics and Materials*, 554, pp. 520-525.
6. Khalid, A., Suardi, M., Chin, R.Y.S., Amirnordin, S.H., "Effect of Biodiesel-water-air Derived from Biodiesel Crude Palm Oil Using Premix Injector and Mixture Formation in Burner Combustion", (2017) *Energy Procedia*, 111, pp. 877-884.
7. Osman, S. A., Alimin, A. J., & Liang, V. S. (2013). Optimum Combustion Chamber Geometry for a Compression Ignition Engine Retrofitted to Run Using Compressed Natural Gas (CNG). In *Applied Mechanics and Materials* (Vol. 315, pp. 552–556). Trans Tech Publications, Ltd. <https://doi.org/10.4028/www.scientific.net/amm.315.552>
8. Alimin, A., Roberts, C., and Benjamin, S., "A NOX Trap Study Using Fast Response Emission Analysers for Model Validation," *SAE Technical Paper 2006-01-0685*, 2006, <https://doi.org/10.4271/2006-01-0685>
9. Wei, T.C., Selamat, H., Alimin, A.J. Modeling and control of an engine fuel injection system (2010) *International Journal of Simulation: Systems, Science and Technology*, 11 (5), pp. 48-60.
10. Fukuda K. (2012). Numerical Simulation of Fuel Sprays in Diesel Engines. Electronic Theses and Dissertation, Ph.D Thesis.
11. G. A (2012). *Numerical Simulation of Ultra-High Injection Diesel and Biodiesel Fuel Sprays*. Electronic Theses and Dissertation, Ph.D Thesis.
12. Iaccarino G. (2001). Predictions of a Turbulent Separated Flow Using Commercial CFD Codes. *Journal of Fluids Engineering*, Vol. 123, pp. 819– 828.
13. Li T., Gel A., Pannala S., Shahnama M., and Syamlal M. (2014). CFD simulations of circulating fluidized bed risers, part I: Grid study. *Powder Technology*, Vol 254, p. 170–180.
14. Longest P.W., and Vinchurkar S. (2007). Effects of mesh style and grid convergence on particle deposition in bifurcating airway models with comparisons to experimental data. *Medical Engineering & Physics*, Vol 29, p. 350–366.
15. Khalid A. (2011). A Study on Effects of Mixture Formation on Ignition and Initial Heat Release of Diesel Spray. *International Journal of Mechanical, Aerospace, Industrial, Mechatronic and Manufacturing Engineering*, Vol 6.
16. Hwang R. D., Liu S.S., and Reitz Z. (1996). Breakup Mechanisms and Drag Coefficients of HighSpeed Vaporizing Liquid Drops. *Atomization of Sprays*, Vol. 6, pp. 353–376.